Original scientific paper

MODELING OSTEOCYTE UNDER SHOCK-WAVE THERAPEUTIC LOADING

Alexey Smolin, Galina Eremina

Institute of Strength Physics and Materials Science SB RAS, Tomsk, Russia

Abstract. *Dental implants have substantial significance in modern dentistry, but their osseointegration stage remains the most crucial and time-consuming step for compensating for a lost tooth. One promising approach to improve osseointegration rates is the use of extracorporeal shock wave therapy, which has shown efficacy in treating fractures, bone defects, and bone tissue regeneration in surgical and arthroplasty procedures. To comprehend the potential of shock wave therapy in accelerating implant osseointegration, it is crucial to investigate the influence of mechanical loading on ossification processes of varying scales objectively. This study aims to study numerically the effects of low-energy shock wave therapy at different intensities on the mechanical response of a single osteocyte, the principal bone cell that corresponds to microscale of bone tissue. The investigation employs the method of movable cellular automata for modeling. The computer simulation results and analysis based on mechanobiological principles indicate that low-intensity shock wave loading creates conditions for intramembranous ossification, whereas high-intensity shock wave exposure creates conditions for endochondral ossification.*

Key words: *Dental implant, Osseointegration, Bone tissue, Osteocyte, Shock-wave therapy, Mechanobiological principles*

1. INTRODUCTION

Dental implants are becoming an increasingly common procedure to restore the functionality of the human teeth and oral health. The most time-consuming and important stage of the installation of a dental prosthesis is the osseointegration of its metal implant with the bone tissue. Therefore, an important task is to find a way to speed up this process.

It should be noted here that osseointegration as well as fracture healing are possible due to the fact that in the bones of a healthy body there is a permanent process of destruction

of old tissues by special cells (osteoclasts) and creation of new tissues by other cells (osteoblasts), which is referred to as remodeling.

The first in vivo and in situ studies of the processes of osseointegration of implants in animals were conducted in 1952 [1]. Later microscopic studies of a microcirculation and intravascular behavior of human blood cells near titanium implants on the arms of healthy volunteers revealed no inflammatory processes. The first dental implants for humans were installed in 1965.

As a result of numerous studies conducted since then, scientists have come to the conclusion that osseointegration of a dental implant occurs according to the scenario of differentiation of osteoprogenitor cells (osteogenic cells, mesenchymal stem cells) into osteoblasts with subsequent intramembranous ossification, i.e., without the formation of cartilage tissue [2, 3]. It should be noted that the second type of ossification, endochondral ossification, which occurs inside cartilage germs when progenitor cells differentiate into chondroblasts, is typical of fracture healing. At the same time, many authors note that the main stages of the process of dental implant osseointegration in the jaw tissues take place at the scale of hormones, proteins, and cells (micro-scale) [4, 5]. Moreover, the surface properties of the implant and new methods of surface treatment additionally stimulate the osteogenic cell response [6, 7]. Another possible mechanism for stimulating cell response is the use of electrical signals, which can be generated, for example, by piezoelectric scaffolds [8] that are specially designed and manufactured using additive technologies [9, 10].

The process of osseointegration during dental implant placement at the micro- and mesoscale (characterized by the structure of the formed tissues) is similar to primary bone healing [3]. Initially, blood and tissue fluid are present between the implant and the bone, and a blood clot is formed. The blood clot is engulfed by phagocytic cells such as polymorphonuclear leukocytes, lymphoid cells, and macrophages. As a result of cellular activity, the implant surface is covered with a protein layer, the structure and composition of which are determined by the type of surface. In this layer, cell adhesion, migration, and differentiation begin, which promote the interaction of cells with the implant surface over several hours or days. At the next stage, connective tissue similar to fibrous tissue is formed, up to 4 mm thick [11]. Further, under the action of external mechanical loads (which are always present due to physiological activity) in the connective tissue, there is a differentiation of cells into osteoblasts and fibroblasts, which are the basis for bone synthesis: the main cells of bone tissue—osteocytes, collagen, and extracellular matrix. After that, the phase of bone callus comes, where the number of osteoblasts increases. Further, under the influence of mechanical load, woven bone is formed, which possesses reduced mechanical characteristics compared to healthy tissue. At the very last stage, woven bone is transformed into healthy (lamellar) bone tissue [12, 13].

According to mechanobiological principles, mechanical stresses and strains affect bone tissue remodeling as follows [14, 15]. Hydrostatic pressure with a magnitude of up to 0.15 MPa and a shear strain value of up to 5% promotes intramembranous ossification (formation of osteoblasts), which leads to the formation of cortical and spongy bone tissue. At values of compressive stresses above 0.15 MPa and strains greater than 5%, endochondral ossification takes place (formation of chondrocytes and cartilage tissue). Compressive stresses of the order of 0.7–0.8 MPa are the most favorable for cartilage tissue formation. At tensile stresses higher than 0.15 MPa with a strain of more than 5%, processes of fibrous tissue formation occur. At stresses lower than 0.003 MPa,

chondroginesis and osteogenesis do not occur. In addition, it was shown by Gardinier et al. [18] that the pore pressure of interstitial fluid in the range of 20 kPa to 2 MPa (68 kPa is the most favorable value) is considered optimal for the development of osteoblasts. At strains of less than 1%, osteoclasts develop, and, as a consequence, bone tissue resorption occurs.

To accelerate the process of osseointegration, non-invasive methods are currently being developed, which are divided into drug therapy and external mechanical treatment. Currently, there are active studies based on mechanobiological principles to investigate the influence of external mechanical factors on the processes of osseointegration of dental implants at the micro- and mesoscopic scales [19]. So Borzabadi-Farahani [20] and Amid at al. [20, 21] investigated the influence of external low-intensity laser exposure on the processes of proliferation and differentiation of dental mesenchymal cells, including on the implant surface.

To increase the speed and quality of osseointegration, it looks promising to use extracorporeal shockwave therapy, which has proven itself for the treatment of fractures and a number of diseases of the musculoskeletal system. The therapeutic effect of shockwave therapy in dentistry is being actively investigated for the treatment of dental caries and parandanthosis [22, 23] and regeneration of alveolar bone tissue in common degenerative diseases [24, 26]. Since 2010, the possibilities of using shockwave therapy before and after implant placement in the dental area have been actively investigated [27, 28].

Bone remodeling is known to be regulated by osteocytes. Osteocytes are the main cells of bone tissue and are located in lacunae (bone cavities) surrounded by the perilacunar matrix (PCM), embedded, in turn, in the bone matrix (or extracellular matrix, ECM). Osteocytes are connected to each other by slender cell processes located within small tubes called the canaliculi. It is believed that osteocytes and canaliculi are peculiar mechanosensors and mechanotransducers that can "sense" mechanical loads and convert them into biochemical signals that regulate bone remodeling [29, 30, 31].

Thus, to better understand the possibility of using external loadings to accelerate the osseointegration of dental implants, it is important to know what happens under such influences in the main cells of bone—osteocytes.

In turn, it is known that the processes of exchange of nutrients and metabolic products, as well as biochemical signals in osteocytes, depend on the flow of tissue (interstitial) fluid [32]. Basically, nutrients are transported both by the flow of this fluid and by diffusion within the bone [33, 34].

Since the experimental study of the above-mentioned processes in bone tissues at the microscale is a challenge, an effective alternative method for *in vitro* biomechanical studies is computer simulation [35, 36]. In this case, numerical models of the mechanical behavior of bone tissues must necessarily take into account the role of interstitial fluid.

This study aims to investigate of the effects of shockwave therapy in various ranges on the mechanical behavior of osteocytes in the area of implant placement using computer simulation.

2. MODEL DESCRIPTION AND VALIDATION

2.1 Movable Cellular Automaton Method for the Fluid Saturated Materials

To describe the mechanical behavior of bone tissue, herein we used the model of a poroelastic body implemented in the method of movable cellular automata (MCA) [37]. It has been established that this particle method has proven itself to be very promising for modeling the mechanical loading of different materials at the macro- and mesoscale [38, 39, 40]. In the MCA method, a specimen is considered an ensemble of discrete elements of finite size (cellular automata) that interact with each other according to certain rules, which, within the particle approach and due to many-body interaction forces, describe the deformation behavior of the material as an isotropic elastoplastic body. The motion of the ensemble of elements is governed by the Newton-Euler equations for their translation and rotation. Within the framework of the MCA method, the value of the averaged stress tensor in the volume of an automaton is calculated as a superposition of forces that act on the areas of interaction of the automaton with its neighbors [38]. It is assumed that stresses are homogeneously distributed in the automaton volume. Knowing the components of the averaged stress tensor allows adapting to MCA different models of plasticity and fracture in the classical solid mechanics.

Automata simulating fluid-saturated material are considered as porous and permeable. The pore space of such an automaton is presented by pores and channels that can be saturated with fluid. The characteristics of the pore space are taken into account implicitly using the effective integral characteristics, namely, porosity ϕ (including narrow channels), permeability k, ratio $a = 1 - K/K_S$ of the macroscopic value of bulk modulus K to the bulk modulus of the solid skeleton K_S [37]. The mechanical influence of the pore fluid on stresses and strains in the solid skeleton of the automaton is taken into account on the basis of the Biot linear model of poroelasticity. Within the framework of this model, the mechanical response of a "dry" automaton is assumed to be linearly elastic. The mechanical effect of the pore fluid on the behavior of the automaton is described in terms of the local pore pressure P^{pore}, which only affects the diagonal components of the stress tensor. The interstitial fluid is assumed to be linearly compressible and is described by the following equation of state

$$\rho\left(P^{\text{pore}}\right) = \rho_0\left(1 + \left(P^{\text{pore}} - P_0\right)/K_{\text{fl}}\right),$$

where ρ and P^{pore} are the current values of the density and fluid pore pressure in the volume of the automaton; ρ_0 and P_0 are the equilibrium values of fluid density and pressure under atmospheric conditions and K_{fl} is the bulk modulus of the interstitial fluid.

The interstitial fluid filtration in the material is governed by Darcy's law

$$\phi\frac{\partial\rho}{\partial t} = K_{\text{fl}}\nabla\left[\frac{k}{\eta}\nabla\rho\right],$$

where η is the fluid viscosity and k is the permeability coefficient of the solid skeleton, which depends on porosity as $k = \phi d_{\text{ch}}^2$ where d_{ch} is the diameter of filtration channel.

2.2 Description of the Model, Its Verification and Validation

To investigate the influence of dynamic loading on mechanosensory effects during bone tissue remodeling, numerical models describing the flow of interstitial fluid in a mesoscopic unit of cortical tissue, the osteon, have recently been actively developed, taking into account the systems of canaliculi and lacunae of the microscopic unit of bone tissue, the osteocyte [41, 42]. Wang et al. [43] presented a more detailed poroelastic model of a single osteocyte in the extracellular matrix.

Within the framework of this study, a three-dimensional model of the main segment of the osteon—the osteocyte—was developed to investigate the influence of shock wave exposure on osseointegration during implant placement. The material parameters of the main parts of the osteocyte and its geometrical characteristics corresponded to the data presented by Wang et al. [43]. The study of dynamic loading with different shock wave parameters on the mechanical behavior of a single osteocyte, taking into account its structural features, is proposed.

We considered an idealized model that consisted of an oval-shaped osteocyte cell body, canaliculi, and cell processes placed in a cube-shaped ECM matrix (Figs. 1, 2). The side length of each direction of the ECM cube corresponded to the literature data for humans and is 43 μm [44]. The canaliculi were tubular structures with an outer layer of PCM with a thickness of ~0.5–1 μm [45] and an inner content of cylindrical channels with a diameter of 0.25 μm, whose physical and mechanical properties were similar to those of the material of the osteocyte body [44].
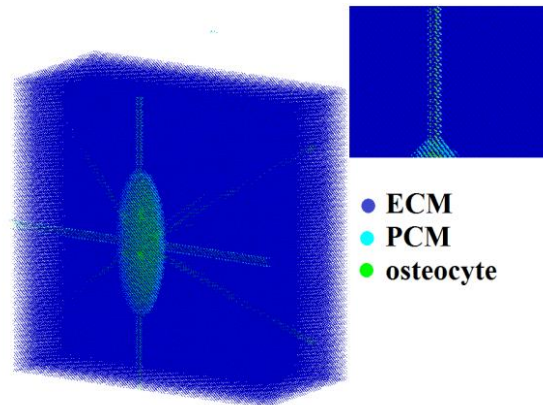

Fig. 1 A half of model osteocyte specimen (section) with indication of materials

The poroelastic model of biological materials was characterized by the following parameters: density (ρ), bulk modulus (K), bulk modulus of the solid phase of the material (K_s), shear modulus (G), porosity (φ), and permeability (k). The properties of biological materials used in the model are presented in Table 1. The biological fluid inside the materials had the properties of salt water with the bulk modulus $K_f = 2.4$ GPa, the density $\rho_f = 1000$ kg/m3, and the viscosity $\eta_f = 1$ mPa·s.

Table 1 Properties of the materials

Material	Density, kg/m^3	Bulk modulus, MPa	Bulk modulus of solid phase, MPa	Shear modulus, GPa	Porosity	Permeability, 10^{-20} m^2
ECM	1850	18300	19000	3.59	0.06	1
PCM	1000	0.0667	0.2668	0.0142	0.75	4
Osteocyte	1000	0.00516	0.0258	0.001107	0.80	6

The initial conditions represent the equilibrium configuration of the system of automata (particles) in the absence of deformations and stresses (i.e., all forces between automata are zero). The fluid content in biological tissues corresponds to the pore volume and zero pressure.

For verification and validation of the osteocyte model, uniaxial compression of the model specimen was simulated (Fig. 2, a); for the main studies, shock wave loading with different parameters was simulated (Fig. 2, b).

The boundary conditions corresponded to the chosen scheme of loading: the lower layer of automata was rigidly fixed (their velocities were set equal to zero, as shown in Fig. 2), and the automata of the upper layer moved along the vertical axis of loading. The value of the Z-component of velocity of the upper layer was constant and equal to 1 mm/s in the case of uniaxial compression (Fig. 2,a) and was changed in time according to the specified energy flux density (EFD) of the shock wave (see [39] for the detailed description of the loading velocity computation) in the case of shock-wave loading (Fig. 2,b). The lateral boundaries of the specimen are free. Temperature effects were not accounted for in the calculations.
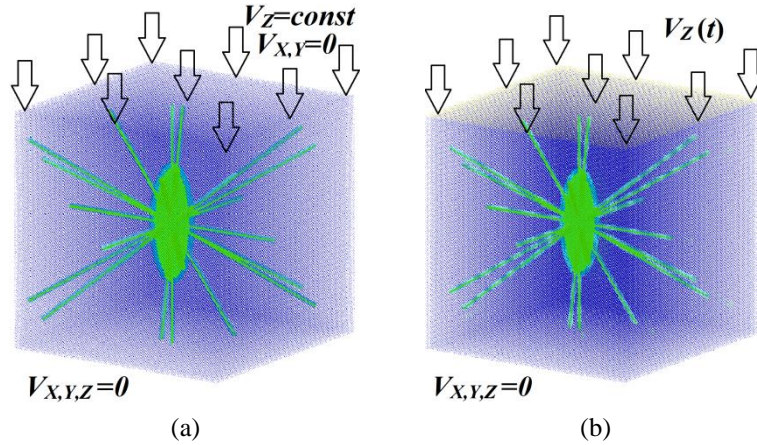

(a)   (b)

Fig. 2 Boundary conditions for modeling uniaxial compression (a) and shock wave loading (b) of the model osteocyte specimen

The main purpose of verification is to check the efficiency of the numerical scheme for solving the governing equations of the method. The main means of model verification is the analysis of the convergence of the obtained results with increasing discretization. Discretization of the domain is considered optimal when further increases in the model resolution lead to a change in the solution of no more than 5%. In this paper, the convergence analysis of a three-dimensional osteocyte model was performed for the system stiffness (integral parameter) at different discretizations of the considered domain, i.e., the size of the discrete element. The number of automata (discrete elements) in the model varied from 1239752 to 4141898 (the size of automata varied from 0.5 to 0.3 μm, respectively).

The results on the convergence of the model stiffness showed that the maximum difference in the stiffness value between the minimum and maximum discretization did not exceed 2%, and it was less than 0.1% for the two extreme values of the automaton size (Fig. 3). Such a small difference indicates a good convergence of the numerical model. The smallest difference in the value of the effective stiffness of the system is observed for 2692237 and 4141898 automata. At the same time, the computational times for these systems are 5 and 12 hours. Therefore, the sample with the number of automata equal to 2692237 was chosen as optimal for the further calculations.
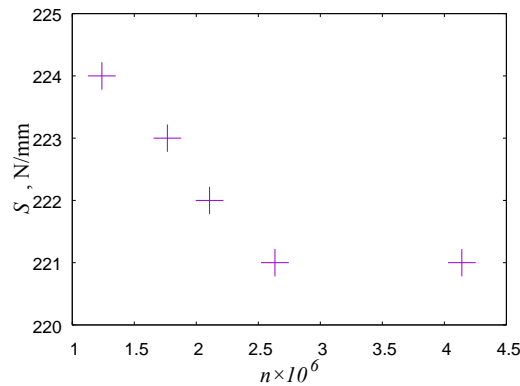

Fig. 3 Dependence of stiffness of a model osteocyte specimen on the number of automata

Validation of the developed osteocyte model was performed by comparing the modeling results with literature data [43]. Uniaxial compression of the model specimen with different loading rates was considered, and the distribution of fluid pressure in the pores and its maximum value were analyzed (Fig. 4).

The analysis of the obtained results showed that at a strain of 1.5×10^{-4}, the maximum value of the analyzed parameter is 80 kPa at a velocity of 100 mm/s, 50 kPa at 10 mm/s, 20 kPa at 1 mm/s, 9 kPa at 0.1 mm/s, and 8.7 kPa at 0.01 mm/s. Thus, it is shown that the osteocyte model under consideration is highly sensitive to loading rate. Moreover, at loading rates of 0.1 and 0.01 mm/s, the maximum value of fluid pressure in the pores corresponds to the values of this parameter presented by Wang et al. [43] under similar loading.
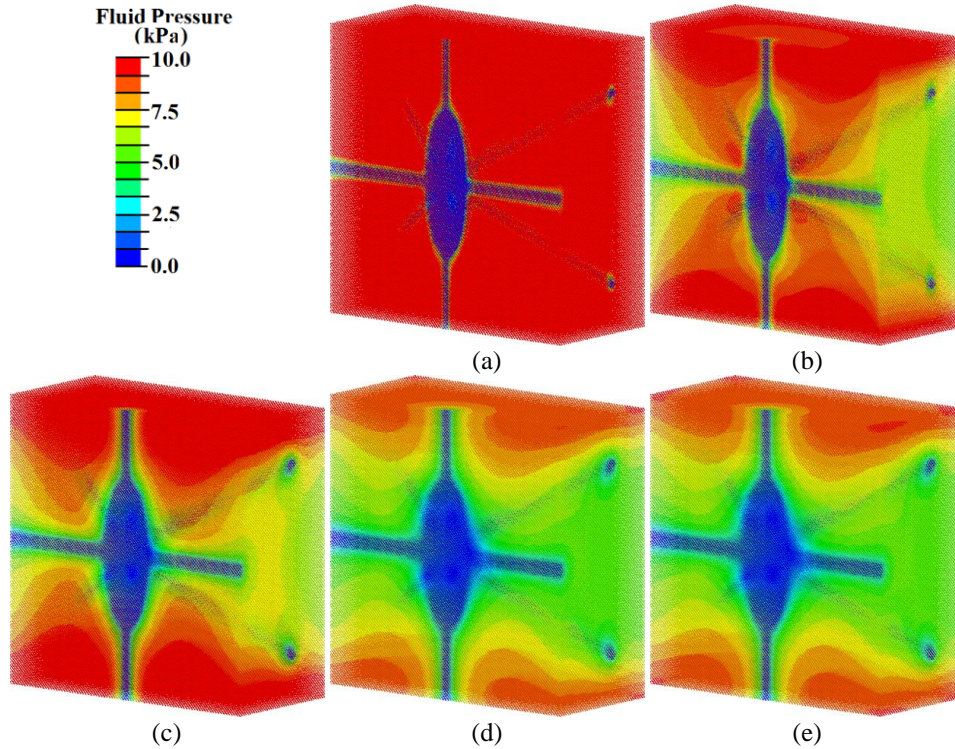
Fig. 4 Pore fluid pressure distribution for a model osteocyte specimen at an engineering strain of 1.5×10^{-4} under uniaxial compression with different loading rates: 100 mm/s (a), 10 mm/s (b), 1 mm/s (c), 0.1 mm/s (d), 0.01 mm/s (e)

3. SIMULATION OF SHOCK WAVE LOADING OF OSTEOCYTE

Most of the works on the numerical study of the mechanical behavior of the structural unit of bone tissue are devoted to static loads [42, 46, 47]. Sathishkumar et al. [25] showed that the regenerative effect of shock wave therapy on bone remodeling around the tooth is observed at an exposure with an energy flux density (EFD) of 100 kJ/mm^2. Therefore, herein, we studied the low-intensity acoustic effect of the shock wave within the range of EFD from 30 up to 170 kJ/mm^2. It is worth noting that the time of pressure increase for such a load is comparable to the characteristic time of interstitial fluid filtration in the studied system.

The hydrostatic pressure fields (Fig. 5,a, where compression corresponds to negative values) show that under low-intensity shock-wave loading (energy flux density of 40 kJ/mm^2), there were areas in the extracellular matrix of the model specimen with compression stresses higher than the minimum values necessary for osteogenesis activation (3 kPa), and the threshold values at which chondrocyte differentiation occurs (less than 0.15 MPa) were not observed. In the area of the osteocyte and its outgrowths, the

compression stress was about 50 kPa. Such values of hydrostatic pressure contribute to the differentiation of osteoblasts.
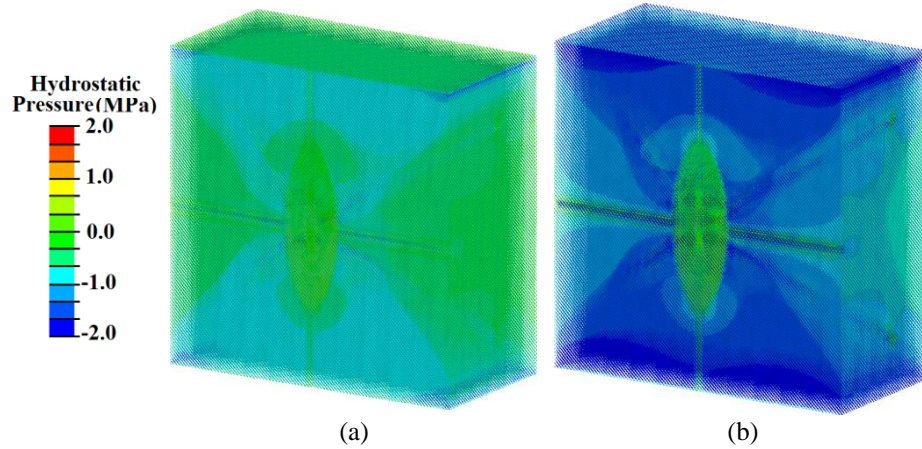

(a)   (b)

Fig. 5 Distribution of hydrostatic pressure in the model specimen under shock wave loading with an energy flux density of 40 kJ/mm^2 (a) and 168 kJ/mm^2 (b)

When the osteocyte model was loaded with a high-intensity shock wave with an energy flux density of 168 kJ/mm^2, areas with compressive stresses of more than 0.15 MPa were observed in the ECM region (Fig. 5,b), which is a condition for cartilage tissue development.
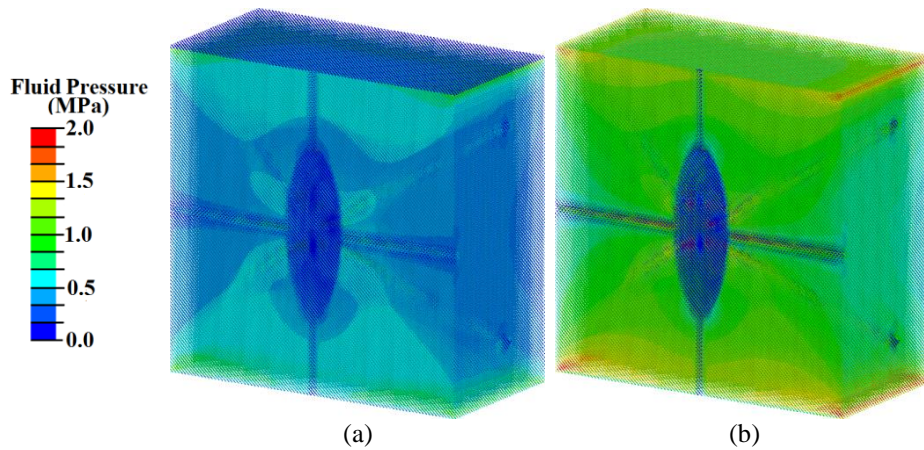

(a)   (b)

Fig. 6 Distribution of pore fluid pressure in the model specimen under shock wave loading with an energy flux density of 40 kJ/mm^2 (a) and 168 kJ/mm^2 (b)

From the analysis of the pressure fields of interstitial fluid (Fig. 6), it was found that at low and high-intensity loading in the area of the extracellular matrix, osteocyte canaliculi,

and osteocyte shell, the necessary level of tissue fluid pressure is observed to trigger the processes of biological cell transfer (more than 68 kPa).
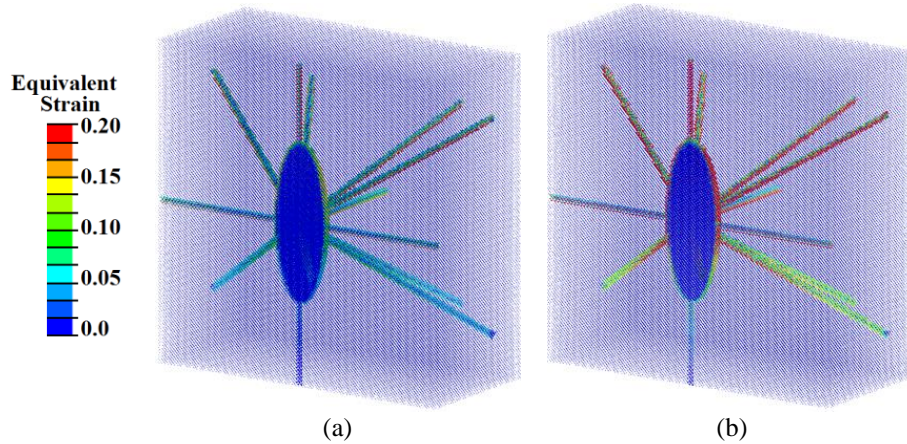

(a)   (b)

Fig. 7 Distribution of equivalent strain in the model specimen under shock wave loading with an energy flux density of 40 kJ/mm^2 (a) and 168 kJ/mm^2 (b)

Now let us consider the equivalent strain fields in the osteocyte model under shock wave loading. As can be seen from Fig. 7, a, under low-intensity loading, the strain level is about 0.5% in the ECM, about 5% in the osteocyte shell, and about 10% in the canaliculi. The maximum strain values (about 20%) are concentrated in the canaliculi near the loading region. According to mechanobiological principles, such values favor the differentiation of osteoclasts and the formation of gaps in the extracellular matrix. However, at large deformations, the osteocyte signals the surrounding tissues to start the process of differentiation of osteoblasts, which serve as the main cells promoting bone tissue growth.

4. DISCUSSION

A numerical model of the mechanical behavior of the main structural unit of the osteon—an osteocyte with canaliculi surrounded by extracellular matrix—was developed on the basis of the movable cellular automaton method, which was verified and validated.

Analysis of the modeling results according to the mechanobiological principles allowed us to reveal that the conditions for intramembranous ossification are created at low-intensity shock-wave loading. At high-intensity shock-wave exposure conditions, the conditions for endochondral ossification are created. The endochondral ossification at the early stages of dental implant healing was also described by Kung et al. [48] and Li et al. [49].

Irandoust and Müftü [19] noted that a large gap between the implant surface and bone tissue promotes the formation of soft tissue (cartilage), which in turn is a negative phenomenon in the process of osseointegration. Babayi et al. [50] showed using modeling that the application of loading immediately after implant placement promotes the growth of fibrous cartilage tissue around the implant in the early stages of osseointegration. While

delayed loading (only the neighboring teeth were loaded and the implant itself was not loaded) promotes more active bone growth in the early stages.

It follows from the analysis of literature that at the early stages of osseointegration, fibrocartilaginous tissue may appear, which later differentiates into bone tissue, and this is a manifestation of endochondral ossification. Such conclusions, based on the results of numerical calculations, including the results of this work, contradict the basic idea that the osseointegration of the dental implant occurs by the intramembranous type of ossification. *In vivo* studies have shown that fibrous tissues can promote osteoblast adhesion by utilizing type I collagen to form the extracellular matrix [51]. This may even promote the migration of osteogenic cells from the surrounding bone to the implant and thereby help to increase the rate of osseointegration [52, 53, 54]. Since fibroblasts may play a dual role in osseointegration, the authors of [51] concluded that restricted fibroblast colonies promote osteogenic cell differentiation, thereby promoting the osseointegration of dental implants.

5. CONCLUSIONS

Despite the fact that endochondral ossification is not typical for osseointegration, the data obtained from the calculations performed and the literature review confirm that the presence of small areas of cartilage occurs during the placement of a dental implant and their role in the subsequent establishing of a functional connection between the dental implant and bone should be considered and further studied.

A micromodel of the main structural unit of the osteon presented herein as well as a macromodel of the jaw segment with a dental implant presented by the authors [55] allow multiscale numerical study of the use of shock-wave exposure to control and accelerate the osseointegration of jaw tissues during dental implant placement.

REFERENCES

1. Jayesh, R.S., Dhinakarsamy, V., 2015, *Osseointegration*, Journal of Pharmacy and Bioallied Sciences, 7(1), pp. S226-S229.
2. Boonsiriseth, K., Suriyan, N., Min, K., Wongsirichat, N., 2014, *Bone and soft tissue healing in dental implantology*, Journal of Medicine and Medical Science, 5(5), pp. 121-126.
3. Pandey, C., Rokaya, D., Bhattarai, B.P., 2022, *Contemporary concepts in osseointegration of dental implants: A review*, BioMed Research International, 2022, 6170452.
4. Brånemark, P.I., 2005, *The osseointegration book: from calvarium to calcaneus*, Quintessence, Berlin 494 p.
5. Cooper, L.F., Shirazi, S., 2022, *Osseointegration—the biological reality of successful dental implant therapy: A narrative review*, Frontiers of Oral and Maxillofacial Medicine, 4, 39.
6. Palmquist, A., Omar, O.M., Esposito, M., Lausmaa, J., Thomsen, P., 2010, *Titanium oral implants: surface characteristics, interface biology and clinical outcome*, Journal of the Royal Society. Interface, 7, pp. S515-S527.
7. Xie, J., Rittel, D., Shemtov-Yona, K., Shah, F.A., Palmquist, A., 2021, *A stochastic micro to macro mechanical model for the evolution of bone-implant interface stiffness*, Acta Biomaterialia, 131, pp. 415-423.
8. Badali, V., Checa, S., Zehn, M., Marinkovic, D., Mohammadkhah, M., 2023, *Computational design and evaluation of the mechanical and electrical behavior of a piezoelectric scaffold: A preclinical study*, Frontiers in Bioengineering and Biotechnology, 11, 1261108.
9. Stojkovic, J., Stojkovic, M., Turudija, R., Arandelovic, J., Marinkovic, D., 2023, *Adjustable elasticity of anatomically shaped lattice bone scaffold built by electron beam melting Ti6Al4V powder*, Metals, 13(9), 1522.

10. Turudija, R., Stojkovic, M., Stojkovic, J., Arandelovic, J., Marinkovic, D., 2024, *Stiffness of anatomically shaped lattice scaffolds made by direct metal laser sintering of Ti-6Al-4V powder: A comparison of two different design variants*, Metals, 14(2), 219.

11. Hermann, J.S., Buser, D., Schenk, R.K., Higginbottom, F.L., Cochran, D.L., 2000, *Biologic width around titanium implants. A physiologically formed and stable dimension over time*, Clinical Oral Implants Research, 11, pp. 1-11.

12. von Wilmowsky, C., Moest, T., Nkenke, E., 2014, *Implants in bone: Part I. A current overview about tissue response, surface modifications and future perspectives*, Oral and Maxillofacial Surgery, 18, pp. 243-257.

13. Guglielmotti, M.B., Olmedo, D.G., Cabrini, R.L., 2019, *Research on implants and osseointegration*, Periodontology 2000, 79(1), pp.178-189.

14. Wang, M., Yang, N., Wang, X., 2017, *A review of computational models of bone fracture healing*, Medical and Biological Engineering and Computing, 55(11), pp. 1895-1914.

15. Claes, L.E., Heigele, C.A., 1999, *Magnitudes of local stress and strain along bony surfaces predict thecourse and type of fracture healing*, Journal of Biomechanics, 32, pp. 255-266.

16. Giori, N.J., Ryd, L., Carter, D.R., 1995, *Mechanical influences on tissue differentiation at bone—cement interfaces*, The Journal of Arthroplasty, 10(4), pp. 514-522.

17. Carter, D.R., Beaupré, G.S., Giori, N.J., Helms, J.A., 1998, *Mechanobiology of skeletal regeneration*, Clinical Orthopaedics and Related Research, 355S, pp. S41-S55.

18. Gardinier, J.D., Majumdar, S., Duncan, R.L., Wang, L., 2009, *Cyclic hydraulic pressure and fluid flow differentially modulate cytoskeleton re-organization in MC3T3 osteoblasts*, Cellular and Molecular Bioengineering, 2(1), pp. 133-143.

19. Irandoust, S., Müftü, S., 2020, *The interplay between bone healing and remodeling around dental implants*, Scientific Reports, 10, 4335.

20. Borzabadi-Farahani, A., 2016, *Effect of low-level laser irradiation on proliferation of human dental mesenchymal stem cells; a systemic review*, Journal of Photochemistry and Photobiology. B, Biology, 162, pp. 577-582.

21. Amid, R., Kadkhodazadeh, M., Gilvari Sarshari, M., Parhizkar, A., Mojahedi, M., 2022, *Effects of two protocols of low-level laser therapy on the proliferation and differentiation of human dental pulp stem cells on sandblasted titanium discs: An in vitro study*, Journal of Lasers in Medical Sciences, 13, e1.

22. Venkatesh Prabhuji, M.L., Khaleelahmed, S., Vasudevalu, S., Vinodhini, K., 2014, *Extracorporeal shock wave therapy in periodontics: A new paradigm*, Journal of Indian Society of Periodontology, 18(3), pp. 412-415.

23. Datey, A., Thaha, C.S.A., Patil, S.R., Gopalan, J., Chakravortty, D., 2019, *Shockwave therapy efficiently cures multispecies chronic periodontitis in a humanized rat model*, Frontiers in Bioengineering and Biotechnology, 7, 382.

24. Falkensammer, F., Arnhart, C., Krall, C., Schaden, W., Freudenthaler, J.W., Bantleon, H.P., 2014, *Impact of extracorporeal shock wave therapy (ESWT) on orthodontic tooth movement—a randomized clinical trial*, Clinical Oral Investigations, 18, pp. 2187-2192.

25. Sathishkumar, S., Meka, A., Dawson, D., House, N., Schaden, W., Novak, M.J., Ebersole, J.L., Kesavalu, L., 2008, *Extracorporeal shock wave therapy induces alveolar bone regeneration*, Journal of Dental Research, 87(7), pp. 687-691.

26. Falkensammer, F., Rausch-Fan, X., Schaden, W., Kivaranovic, D., Freudenthaler, J., 2015, *Impact of extracorporeal shockwave therapy on tooth mobility in adult orthodontic patients: a randomized single-center placebo-controlled clinical trial*, Journal of Clinical Periodontology, 42(3), pp. 294-301.

27. Li, X., Chen, M., Li, L., Qing, H., Zhu, Z., 2010, *Extracorporeal shock wave therapy: A potential adjuvant treatment for peri-implantitis*, Medical Hypotheses, 74(1) pp. 120-122.

28. Elisetti, N., 2021, *Extracorporeal shock wave therapy (ESWT): An emerging treatment for peri-implantitis*. Medical Hypotheses, 150, 110565.

29. Bonewald, L.F., 2011, *The amazing osteocyte*, Journal of Bone and Mineral Research, 26(2), pp. 229-238.

30. Fotia, C., Messina, G.M.L., Marletta, G., Baldini, N., Ciapetti, G., 2013, *Hyaluronan-based pericellular matrix: substrate electrostatic charges and early cell adhesion events*, European Cells and Materials, 26, pp. 133-149.

31. Klein-Nulend, J., Bakker, A.D., Bacabac, R.G., Vatsa, A., Weinbaum, S., 2013, *Mechanosensation and transduction in osteocytes*, Bone, 54(2), pp. 182-190.

32. Cardoso, L., Fritton, S.P., Gailani, G., Benalla, M., Cowin, S.C., 2013, *Advances in assessment of bone porosity, permeability and interstitial fluid flow*, Journal of Biomechanics, 46(2), pp. 253-265.

33. Fritton, S.P., Weinbaum, S., 2009, *Fluid and solute transport in bone: flow-induced mechanotransduction*, Annual Review of Fluid Mechanics, 41, pp. 347-374.

34. Lovett, M., Lee, K., Edwards, A., Kaplan, D.L., 2009, *Vascularization strategies for tissue engineering*, Tissue Engineering Part B: Reviews, 15(3), pp. 353-370.

35. Podshivalov, L., Fischer, A., Bar-Yoseph, P.Z., 2014, *On the road to personalized medicine: multiscale computational modeling of bone tissue*, Archives of Computational Methods in Engineering: State-of-the-Art Reviews, 21 (4), pp. 399-479.

36. Milovanović, J., Stojković, M., Trifunović, M., Vitković, N., 2023, *Review of bone scaffold design concepts and design methods*, Facta Universitatis-Series Mechanical Engineering, 21, pp. 151-173.
37. Smolin, A., Eremina, G., Xie, J., Syrkashev, V., 2022, *Development of a computational model of the mechanical behavior of the L4-L5 lumbar spine: Application to disc degeneration*, Materials, 15(19), 6684.
38. Shilko, E.V., Psakhie, S.G., Schmauder, S., Popov, V.L., Astafurov, S.V., Smolin, A.Yu., 2015, *Overcoming the limitations of distinct element method for multiscale modeling of materials with multimodal internal structure*, Computational Materials Science, 102, pp. 267-285.
39. Smolin, A., Eremina, G., 2023, *Shock-wave impact on the knee joint affected with osteoarthritis and after arthroplasty*, Defence Technology, 20, pp. 1-10.
40. Eremina, G., Smolin, A., Martyshina, I., 2022, *Convergence analysis and validation of a discrete element model of the human lumbar spine*, Reports in Mechanical Engineering, 3(1), pp. 62-70.
41. Yu, W., Wu, X., Cen, H., 2019, *Study on the biomechanical responses of the loaded bone in macroscale and mesoscale by multiscale poroelastic FE analysis*, BioMedical Engineering OnLine, 18, 122.
42. van Tol, A.F., Roschger, A., Repp, F., Chen, J., Roschger, P., Berzlanovich, A., Gruber, G.M., Fratzl, P., Weinkamer, R., 2020, *Network architecture strongly influences the fluid flow pattern through the lacunocanalicular network in human osteons*, Biomechanics and Modeling in Mechanobiology, 19(3), pp. 823-840.
43. Wang, L., Dong, J., Xian, C.J., 2018, *Computational investigation on the biomechanical responses of the osteocytes to the compressive stimulus: A poroelastic model*, BioMed Research International, 2018, 4071356.
44. Gururaja, S., Kim, H.J., Swan, C.C., Brand, R.A., Lakes, R.S., 2005, *Modeling deformation-induced fluid flow in cortical bone's canalicular-lacunar system*, Annals of Biomedical Engineering, 200533(1), pp. 7-25.
45. Beno, T., Yoon, Y.J., Cowin, S.C., Fritton, S.P., 2006, *Estimation of bone permeability using accurate microstructural measurements*, Journal of Biomechanics, 39(13), pp. 2378-2387.
46. Ismail, A.A., Daud, R., Junoh, A.K, Zain, N.A.M., Omar, M.I., Mansor, N.N., 2019, *Effect of lamellae thickness on the stress distribution in single osteon with the presence of lacunae*, Materials Today: Proceedings, 16, pp. 2170-2178.
47. Liu, Y., Li, A., Chen, B., 2020, *Effects of structure characteristics of osteocyte lacunae on squeeze damage resistance of osteons*, Cells Tissues Organs, 208(3-4), pp. 142-147.
48. Kung, P.C., Chien, S.S., Tsou, N.T., 2020, *A hybrid model for predicting bone healing around dental implants*, Materials, 13(12), 2858.
49. Li, M.J., Kung, P.C., Chang, Y.W., Tsou, N.T., 2020, *Healing pattern analysis for dental implants using the mechano-regulatory tissue differentiation model*, International Journal of Molecular Sciences, 21(23), 9205.
50. Babayi, M., Ashtiani, M.N., Emamian, A., Ramezanpour, H., Yousefi, H., Mahdavi, M., 2023, *Peri-implant cell differentiation in delayed and immediately-loaded dental implant: A mechanobiological simulation*, Archives of Oral Biology, 151, 105702.
51. Tamai, M., Harimoto, K., Nagaoka, N., Yoshihara, K., Yoshida, Y., Tagawa, Y.-I., 2021, *Cell adherence competition between osteoblasts and fibroblasts on various materials influences the establishment of osseointegration*, Archives of Clinical and Biomedical Research, 5, pp. 650-663.
52. Shaikhaliyev, A., Polisan, A., Ivanov, S., Parkhomenko, Y., Malinkovich, M., Yarygin, K., Arazashvili, L., 2019, *Effect of the surface of medical titanium endoprostheses on the efficiency of fibrointegration*, Journal of Surface Investigation: X-ray, Synchrotron and Neutron Techniques, 13(4), pp. 644-651.
53. Teng, F.Y., Ko, C.L., Kuo, H.N., Hu, J.J., Lin, J.H., Lou, C.W., Hung, C.C., Wang, Y.L., Cheng, C.Y., Chen, W.C., 2012, *A comparison of epithelial cells, fibroblasts, and osteoblasts in dental implant titanium topographies*, Bioinorganic Chemistry and Applications, 2012, 687291.
54. Aragoneses, J., Suárez, A., López-Valverde, N., Martínez-Martínez, F., Aragoneses, J.M., 2021, *Assessment of the tissue response to modification of the surface of dental implants with carboxyethylphosphonic acid and basic fibroblastic growth factor immobilization (Fgf-2): An experimental study on minipigs*, Biology, 10(5), 358.
55. Smolin, A., Eremina, G., Martyshina, I.,2023, *Simulation of mechanical processes at the contact region of a dental implant with bone tissues under shock wave treatment*, Journal of Materials and Engineering, 1(2), pp. 92–96.